

Enhanced mobility of granular mixtures of fine and coarse particles

J.C. Phillips^{a,b,*}, A.J. Hogg^{a,c}, R.R. Kerswell^{a,c}, N.H. Thomas^d

^a *Centre for Environmental and Geophysical Flows, University of Bristol, Queens Road, Bristol BS8 1RJ, UK*

^b *Department of Earth Sciences, University of Bristol, Queens Road, Bristol BS8 1RJ, UK*

^c *School of Mathematics, University of Bristol, University Walk, Bristol BS8 1TW, UK*

^d *Flow Research Evaluation Diagnostics Ltd, Aston Science Park, Birmingham B7 4BJ, UK*

Received 12 July 2005; received in revised form 24 March 2006; accepted 6 April 2006

Available online 26 May 2006

Editor: V. Courtillot

Abstract

Understanding how granular materials flow remains an outstanding issue in both nature and industry where typically a range of particle sizes are involved. We present laboratory measurements of flows of binary mixtures of fine and coarse granular materials that show that their interaction can result in significantly increased mobility (the ratio of the run out distance for the centre of mass to the initial height of the centre of mass). At a fine material mass fraction ψ (the ratio of the mass of fine particles to the total mass of the flow) of about 0.3, the flow mobility can be increased by up to a factor of 4 compared with the same mass of either all fine or all coarse material. Measurements of the distribution of the deposited fine and coarse particles along the length of the flow show that in low mobility flows the peak in deposition of fine and coarse particles occurs at different positions, whereas for high mobility flows there is a more uniform deposition of both particle sizes. We interpret the observations of flow mobility in terms of two primary mechanisms: at low ψ the fine particles lubricate the flow of the coarse particles by rolling, whereas at high ψ the presence of coarse particles reduces the inter-particle frictional losses in the flow. We use heuristic models to illustrate that these mechanisms are likely to occur in granular flows containing a wide range of grain sizes, noting that the detailed physical descriptions and mathematical models of these particle interactions are currently incomplete. These experimental observations challenge the traditional view that the extent of geophysical granular flows depends on their volume, in line with other recent studies of slumping granular materials. Recent studies which use a single particle size show strong dependence of flow run out on the initial aspect ratio of the release. Our results suggest that compositional effects in flows containing more than one particle size may be at least as important.

© 2006 Elsevier B.V. All rights reserved.

Keywords: granular flow; experiment; rolling; mixtures; segregation; run out length

1. Introduction

Granular flows that occur in nature as rockslides, volcanic block-and-ash pyroclastic flows and dry debris

avalanches, and those arising from industrial processes such as mining and solids conveying, typically contain a range of particle sizes [1–4]. A fundamental process in flows containing more than one particle size or density is segregation; that is, sorting of the particle mixture into regions that are uniform in size or density [5,6]. Segregation can occur due to the movement of smaller particles into the spaces beneath larger particles during shaking [7,8], and large-scale convection within the

* Corresponding author. Department of Earth Sciences, University of Bristol, Queens Road, Bristol BS8 1RJ, UK. Tel.: +44 117 954 5241; fax: +44 117 925 3385.

E-mail address: j.c.phillips@bristol.ac.uk (J.C. Phillips).

granular mixture [9,10], both of which result in the formation of a layer of segregated coarse particles above fine particles, and suggest density-independent rising times for the larger particles. However, recent numerical and experimental studies [11,12] have shown that large particles can segregate to the base of a vibrated bed of particles if sufficiently dense. Particle segregation has also been observed to occur spontaneously during the formation of granular piles from a stream of falling particles, in the absence of any external perturbation [13,14]. Segregation patterns and velocity profiles observed in steady uniform chute flows have led to the development of the *kinetic sieving* model of particle segregation [15] based on a net percolation velocity for the fine particles. This approach gives reasonable agreement between measured and predicted concentration profiles for chute flows of binary particulate mixtures [15,16].

Previous studies have suggested that granular flows containing a range of particle sizes can exhibit macroscale properties that differ from flows containing a single particle size. The minimum energy required to liquefy mixtures of sand, with mean diameter $\sim 240\ \mu\text{m}$, and silt, with mean diameter $\sim 70\ \mu\text{m}$, was found for the mixture with the minimum voidage [17] corresponding to a silt volume fraction of about 0.3 [17,18]. Lubrication effects have also been observed in molecular dynamics simulations of vibrated mixtures of particles of different size and shape formed from co-linear spheres [19]. Segregation of mixtures into layers of a single species was observed, with distinct velocity profiles in each layer. Adding a small number of smaller grains to the larger grains produced a lubrication effect that increased their velocity.

In addition to interactions between the constituent particles of a granular flow with a range of particle sizes, interactions between the particles with the underlying surface also depend on their size. These interactions have been primarily investigated for the case of a single particle on a rough slope [20–23], for which the parameters that control the motion are the particle size relative to the roughness size and the slope angle [21]. A recent experimental study has investigated the dynamics of monodispersed granular flows down inclined roughened surfaces [24]. For a particle size that just filled the roughness spacing, a minimum run out length was observed for the flow, independent of the slope angle. This was interpreted as a state of maximum stability using a geometrical model of a single particle on a rough plane.

Granular flows have been widely studied in a range of experimental continuous shear configurations includ-

ing plane and angular shear flows [25,26], rotating drums [27] and chutes [15,16,24]. A recent synthesis of these experimental observations made by the research group GRD MiDi [28] has led to important new conclusions for the dynamics of dense granular flows. Through identification of appropriate length and time scales for granular motion [28], it is observed that the kinematics of dense granular flow are independent of the microscopic particle roughness and shape. In all experimental geometries, a dense or quasi-static flow regime exists in addition to a dilute collisional regime. Velocity profiles may be localised to regions of high shear (chute flows), linear across the flow (annular shear flow) with the addition of an exponential tail (rotating drum flows). It is suggested that the existence of these different flow regimes results from non-local rheology of dense granular flow, and that the coherence length scale for constant rheological properties may be related to the presence of structures within granular flow such as arches and dense grain clusters [28].

Recently, substantial progress has also been made in examining how granular materials with a narrow size range (*mono-sized particles*) avalanche [29–33]. These studies have used laboratory experiments to investigate the dynamics of the collapse of axisymmetric and two-dimensional granular columns onto a horizontal surface and the subsequent granular flow propagation. The results from these studies challenge the traditional view that the maximum extent of the flow (the *run out distance*) depends only on the volume of material involved in the flow and instead have emphasized the importance of the initial shape or aspect ratio of the material, finding clear power law dependence of the flow run out on the initial aspect ratio of the granular column only.

In this paper we focus on the mobility of a two-species granular flow by conducting a series of laboratory experiments examining the run out length and deposit structure of mixtures of fine and coarse granular materials moving over a rough inclined surface. The flows are ‘stopping flows’, i.e., they flow on slopes that have a gradient less than the angles of friction of the granular materials used. In Section 2, we describe the experimental apparatus and methodology, and in Section 3 we present experimental results documenting the flow run out length, and particle segregation within the flow deposit, for flows consisting of a range of mixtures of coarse and fine particles. In Section 4 we offer heuristic models to interpret the qualitative behaviour of the flows at different fine particle mass fractions. In Section 5 we discuss the experimental results and outline work required to

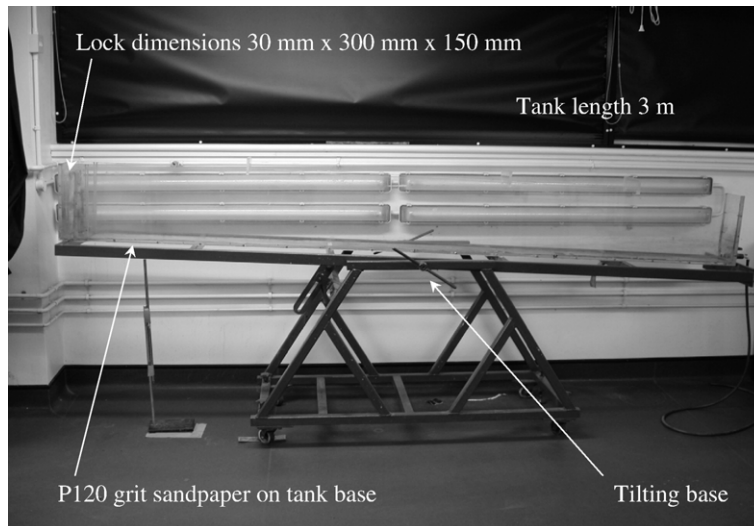


Fig. 1. The two-dimensional inclined tank used in the experiments. The two pairs of horizontal strips are wall-mounted illumination behind the tank.

reconcile experimental and theoretical observations of these flows, finishing by summarising the implications for granular flow motion in Section 6.

2. Experimental method

The laboratory experiments were conducted in a narrow tank, 3 m long \times 150 mm wide, with a lock gate sited 35 mm from one end (see Fig. 1). The tank was mounted on a tilting frame, and was inclined at angles of 10° and 20° to the horizontal in these experiments. Bidisperse mixtures of granular material were released into the tank. These comprised approximately spherical glass ballotini, PVC beads or angular silicon carbide particles as the fine particles, and for most experiments, the coarse material was rectangular glass slabs or sub-spherical sandstone gravel (see Table 1). In preliminary experiments, glass spheres were also used as coarse

particles. For the slope angles and surface roughness investigated here, coarse spherical particles mainly exhibited rolling motion that was independent of the motion of the fine particles. The coarse particles simply rolled to the maximum extent of the experimental apparatus. The exception to this behaviour was observed when the flow consisted of mainly fine particles, in which case the coarse particles were unable to move independently of the flow. In this paper we focus on the motion of binary mixtures of spherical and angular fine particles and angular coarse particles, including comparisons with the motion of mixtures of spherical fine and coarse particles in the limited range of mixture proportions where the flows stopped.

The basal angle of friction of these materials was determined by placing a sample of the fine particles or a representative coarse particle on a small plane whose inclination could be steadily and precisely increased,

Table 1
Experimental materials

Material	Description	Size	Basal friction angle (deg)	Internal friction angle (deg)	Density (kgm^{-3})
140 μm ballotini	Glass spheres	110–140 μm diameter	23	32	2550
90 μm ballotini	Glass spheres	70–110 μm diameter	23	32	2550
140 μm PVC	Sub-spherical beads	110–140 μm diameter	27	33–36	1450
140 μm Silicon Carbide	Angular powder	110–140 μm diameter	27	35	3300
Rafters	Rectangular glass slab	75 mm \times 25 mm \times 2.2 mm	30	–	2550
Double rafters	Rectangular glass slab	75 mm \times 25 mm \times 4.4 mm	30	–	2550
Gravel	Sub-spherical sandstone	10–20 mm diameter	28	–	\sim 2600
Surface roughness	P120 grit glass paper	Mean grit size 127 μm Compactness 0.34 ± 0.025			
Glass spheres		8 mm and 20 mm diameter	<5	<5	2550

and determining the angle at which motion was initiated in the particles. The internal angle of friction of the fine particles was determined by pouring the fine materials into a conical pile, and accurately determining the angle of repose of the pile. In all experiments, the tank inclination was less than the basal and internal angles of friction of the particles used, so that the flows decelerated to rest after the initial gravitational collapse when the lock gate was removed. Experiments were conducted for mixture compositions with a fine material mass fraction ψ ranging from 0 (all coarse) to 1 (all fine).

The base of the inclined tank, the small plane used to determine the static friction angle of the particles and the coarse glass slabs were covered in P120 grit abrasive paper, which consisted of angular silica particles of average size about $127\mu\text{m}$ glued to a smooth paper surface. This material was chosen so that the size of the surface roughness elements was comparable to the fine particle diameter. We used the method of Goujon et al. [24] to determine the surface compactness as 0.34 ± 0.025 , which is the ratio of the projected area occupied by surface roughness elements to the total surface area.

For each experiment, 0.8 kg of a binary mixture consisting of one of the fine particle types and one of the coarse particle types was used. The coarse particles were placed in the lock first. The rectangular glass slabs were arranged with their long axis vertical and their largest face parallel to the plane of the gate (Fig. 2a), whereas the gravel and glass spheres were poured into the lock region to adopt a random configuration (Fig. 2b). The fine particles were then poured into the lock and percolated into spaces between the coarse particles by gravity. After filling the lock, care was taken to not shake the experimental tank to introduce any particle segregation other than that which had occurred on initial pouring. The coarse particles filled the lock region in a close-packed arrangement (Fig. 2). The fine particles occupied the spaces between the coarse particles and at higher fine particle mass fractions (ψ large), completely filled the spaces between the coarse particles and formed an overlying layer. Both layers were uniform along the width and length of the lock, and were clearly visible in the lock region. The mass and height of the layers of fine and coarse particles were known for each mixture combination, so the height of the centre of mass of the mixture could be calculated. We conducted trial experiments with less-ordered initial arrangements of coarse glass slabs by pouring these into the lock; surprisingly, we found that the flow run out length was only weakly dependent on the initial arrangement of fine and coarse material behind the lock gate (maximum

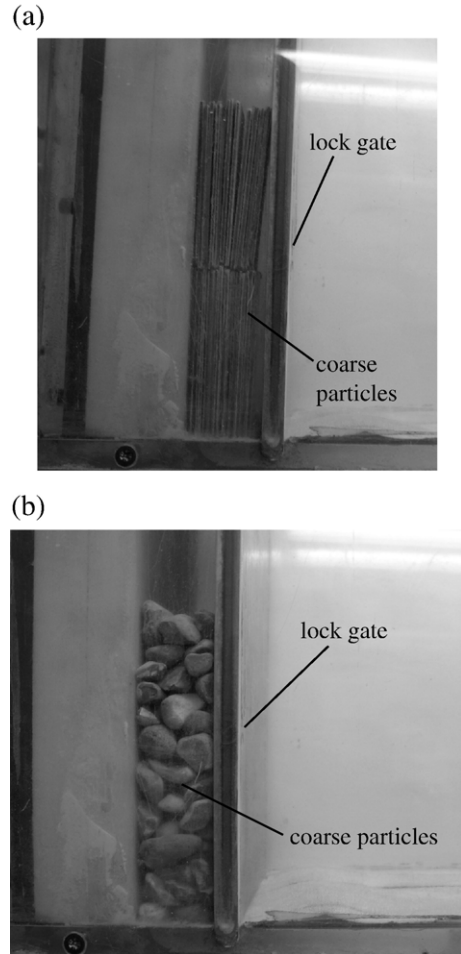


Fig. 2. The initial arrangement of coarse particles in the lock region of the experimental tank: (a) rectangular glass slabs (rafters); (b) gravel.

standard error in run out distance of 8.7% over 5 runs at any mixture proportion). However, in this configuration, the estimate of the initial centre of mass is much less precise, due to high porosity between the coarse glass slabs, so we conducted the experiments using the initial regular arrangement of coarse particles as shown in Fig. 2.

The lock gate was rapidly removed to initiate gravitational collapse of the particle mixture, and this was recorded using video photography. The position of the centre of mass of the deposit was estimated from observations of the deposit made from the side and above. When the flow consisted of mainly coarse or mainly fine particles, the deposit took the form of a low angle wedge of approximately constant slope and with a width equal to that of the channel (Fig. 3). In this case the position of the centre of mass was estimated by assuming that this wedge had a constant porosity, and

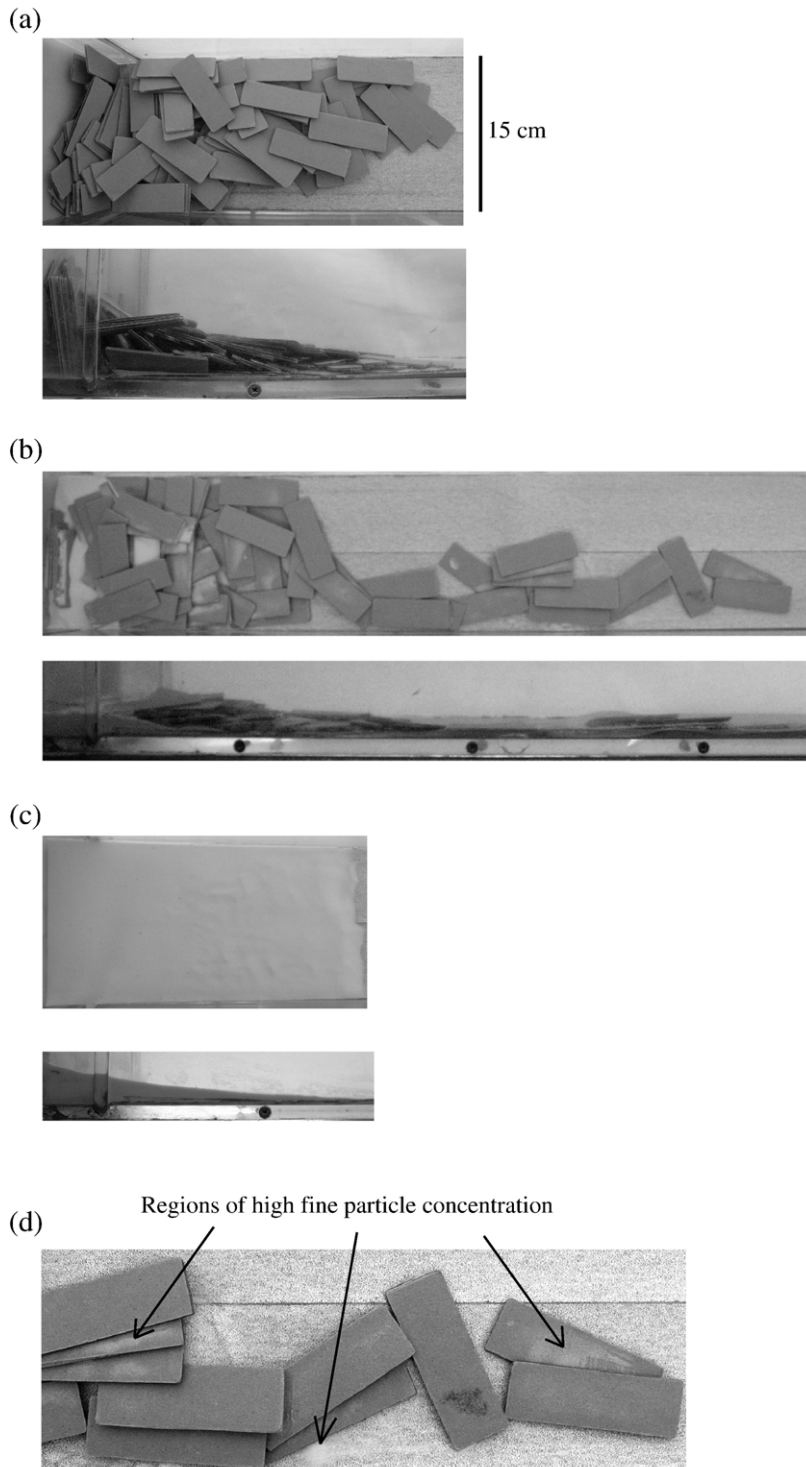


Fig. 3. Photographs of deposits of flows of binary mixtures of flat coarse particles (glass rafters) and fine spherical glass particles ($140\ \mu\text{m}$ glass ballotini) on a 10° slope. Flows propagated from left to right, and photographs (a)–(c) are taken at the same scale. (a) Plan and side view of the flow deposit when the fine particle mass fraction=0. (b) Plan and side view of the flow deposit when the fine particle mass fraction=0.3. (c) Plan and side view of the flow deposit when the fine particle mass fraction=1. (d) Close-up of the deposit front in plan view when the fine particle mass fraction=0.3, showing the fine particles as light coloured powder on the surface of the coarse particles.

image processing software (Image-J, <http://rsb.info.nih.gov/ij/>) was used to identify the centroid. For particle mixtures, an additional thin layer of uniform thickness formed at the front of the deposit (Fig. 3). The volume and centroid of the thin layer and the wedge were determined by image processing of plan and side views, and the centroid of the whole deposit was calculated from these values assuming each had the same porosity. This method was validated with direct measurements of the mass distribution along the deposit made by dividing the deposit into discrete regions along its length and measuring the mass of particles in each region (see Section 3.1). The difference in centroid position determined using these two methods was found to be no more than $\pm 5\%$.

3. Experimental results

3.1. Flow deposits

The profile of the flow deposit along its length and position of individual coarse particles are shown in Fig. 3, which shows side and plan views of the experimental deposit for a binary mixture of $140\mu\text{m}$ ballotini fine particles and coarse glass rafters, at a range of fine material mass fractions. In Fig. 3a, the deposit from a flow consisting of all coarse particles ($\psi=0$) on a 10° slope is shown in plan and side view. The deposit forms an irregular wedge shape, with an angle between the deposit upper surface and the tank base of about 15° . A significant proportion of coarse particles remains within the lock region. In Fig. 3b, the deposit from a flow of a mixture of fine and coarse particles ($\psi=0.3$) on a 10° slope is shown. The deposit profile is much flatter than that of either of the end-member particle mixtures, and the coarse and fine particles are not evenly distributed along the deposit length. In Fig. 3c, the deposit from a flow of all fine particles ($\psi=1$) on a 10° slope is shown. In this case, the deposit forms a uniform wedge typical of deposits from flows containing fine particles with a small range of particle sizes (cf. [34]). The angle between the deposit upper slope and the tank base is about 7.5° , compared with the static friction angle for this material of 23° . Fig. 3d shows a close-up of the distal region of the deposit, in which fine particle deposition can be seen on the surfaces of the coarse particles as well as the base of the tank.

For all binary combinations of fine and coarse particles used in these experiments, the deposits exhibited the following common features. In general, the coarse particles segregated to the upper part of the deposit. In flows that exhibited the greatest run out

length, the region of maximum concentration of coarse particles is further from the flow origin. There appears to be no systematic relationship between the fine particle mass fraction and the number of coarse particles that remain in the initial part of the deposit (within the lock).

In Fig. 4, we show the variation of the mass of fine and coarse particles along the length of the deposit for a binary mixture of $140\mu\text{m}$ ballotini and slab-like glass rafters on 10° and 20° slopes. Mass deposition data is shown for $\psi=0.1, 0.3$ and 0.9 , representative of binary mixtures consisting of mainly coarse particles, the binary mixture proportion which typically exhibited the longest run out, and binary mixtures of mainly fine particles, respectively. Experimental measurements were made for ψ ranging from 0.1 to 1.0 in increments of 0.1, and showed systematic trends across this range that are highlighted in the limited data shown here for clarity. On the 10° slope, the deposit was divided into regions 5 cm in length by inserting two tightly fitting rigid walls across the experimental tank. Coarse particles were removed from this region by hand, and fine particles were removed using a vacuum cleaner from which they were removed and weighed. Loss of fine particles in this process was estimated to be less than 1 g, and the corresponding experimental error is represented by the size of the symbols used in Fig. 4. On the 20° slope, the deposit was divided into regions 10 cm in length.

Figs. 4(a) and (b) show the mass of fine and coarse particles plotted against position in the deposit for flows on 10° and 20° slopes, respectively, with mass fraction of fine particles $\psi=0.1, 0.3$ and 0.9 . The mass of particles is plotted at the position in the deposit that corresponds to the mid-point of the region from which they were collected, and the position 0 cm corresponds to the position of the lock gate. The flow with the greatest run out length ($\psi=0.3$) exhibits flatter profiles of coarse particle mass deposition, and the mass deposition of fine and coarse particles is similar at any given position in the deposit, whereas the mass deposition of fine and coarse particles at any given position in the deposit is dissimilar for binary mixture flows with the shortest run out lengths, corresponding to $\psi=0.1$ and 0.9 (Fig. 4a and b). Experimental measurements for values of ψ between 0.1 and 0.3, and between 0.3 and 0.9 showed monotonic changes in the profile of coarse particle deposition and similarity of mass deposition of fine and coarse particles at the same position in the deposit between the limiting values highlighted in Fig. 4a and b.

Fig. 4c shows the mass deposition of fine particles with distance from the flow origin for binary mixtures

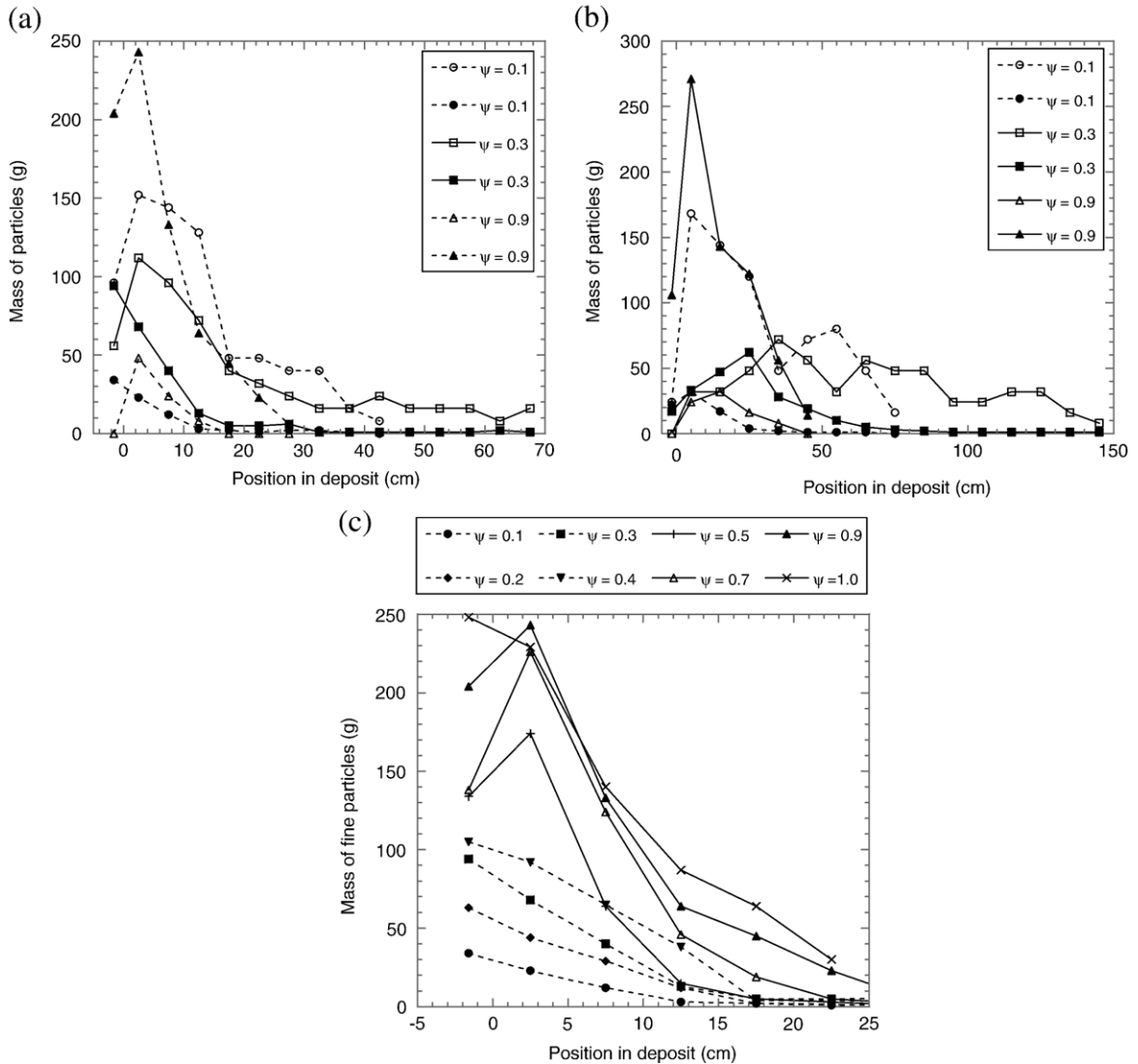


Fig. 4. The variation in mass deposition of fine and coarse particles along the length of the deposit from flows consisting of $140\ \mu\text{m}$ ballotini as the fine particles and slab-like glass rafters as the coarse particles on 10° and 20° slopes. (a) Flows with $\psi = 0.1, 0.3$ and 0.9 on a 10° slope, (b) flows with $\psi = 0.1, 0.3$ and 0.9 on a 20° slope, open symbols show coarse particle deposition and solid symbols show fine particle deposition. (c) The mass deposition of fine particles from flows with ψ from 0 to 1.0. Note that the mass of an individual coarse particle is approximately 8 g. The straight lines joining the data points are for illustrative purposes only. The $\psi = 0.1$ and $\psi = 0.9$ data shows wide disparity in the mass of fine and coarse particles at positions along the length of the deposit, whereas this is similar at $\psi = 0.3$.

with ψ ranging from 0.1 to 1.0 on a 10° slope. Experimental measurements for flows with $\psi = 0.6$ and $\psi = 0.8$ are omitted for clarity, and these data follow the monotonic trend shown in the plotted measurements. There is a systematic trend in the gradient of mass deposition of fine particles with distance from the flow origin, the highest gradient corresponding to the flow with fine particle mass fraction $\psi = 1.0$ and smallest gradient corresponding to the flow with $\psi = 0.1$ (Fig. 4c). In experiments with $\psi < 0.4$, the maximum fine particle

mass deposition is found in the lock region and this monotonically decreases with downstream distance. For all other deposit profiles from flows of binary particle mixtures, the maximum fine particle mass deposition is found further downstream than the lock region. In the deposits from flows with the greatest run out length, a significant mass of fine particles was present in the flow at its front (Figs. 4a, b and 3d). There is no systematic trend in the position of maximum mass deposition of coarse particles, although in general the gradient of the

coarse particle mass deposition profile is greatest for the flows with the greatest proportion of coarse particles (ψ small).

3.2. Flow mobility

Experimental measurements of flow mobility are shown in Fig. 5 for a range of binary mixtures of one fine particle type and one coarse particle type. A

commonly used measure of flow mobility is ratio of the horizontal run out length of the flow (L) to the vertical distance over which it has descended (H ; [35]). However, on a constant slope, this ratio is almost constant, as the only difference in height between experiments is due to different initial heights of the particle bed in the lock, which varies with fine particle mass fraction ψ in our experiments from about 0.09–0.25 m. As this height difference is typically much

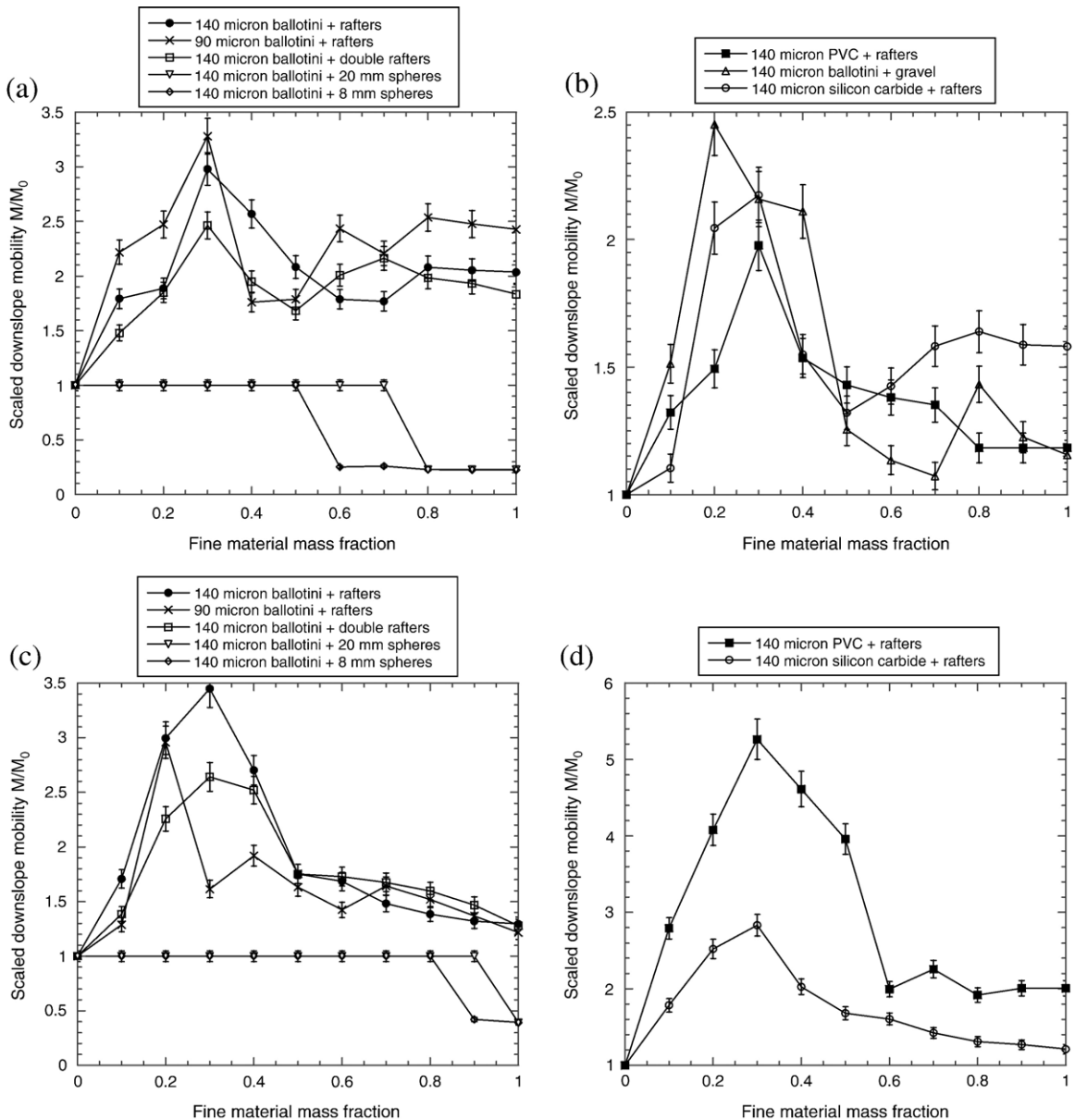


Fig. 5. Downslope mobility of a flow containing a binary mixture of fine and coarse particles on a slope for a range of mixture compositions: (a) and (b) 10° slope; (c) and (d) 20° slope. The error bars show standard error of the mean of 5 experiments, or experimental precision of $\pm 5\%$, whichever is larger. The straight lines joining the data points are for illustrative purposes only.

smaller than the total vertical distance moved by the flow, L/H is not a sensitive measure of the flow mobility in this geometry. A more sensitive measure of the differences in flow mobility is the downslope mobility M , defined here as the ratio of the downslope position of the centre of mass of the mixture deposit to the height of the centre of mass perpendicular to the slope, measured in the lock region prior to removal of the lock gate. To compare experiments at different fine particle mass fractions, we normalised the downslope mobility for each particle mixture by the downslope mobility M_0 of the flow consisting of all coarse material ($\psi=0$). At both slope angles, M/M_0 is significantly increased in experiments using a mixture of fine and coarse particles as compared with experiments using either all fine or all coarse. Even in these small-scale experiments, the downslope mobility can be enhanced by up to a factor of four at $\psi \approx 0.3$. This is a robust phenomenon observed in all our experiments regardless of which fine and coarse particles were used, suggesting that this effect does not depend on the density difference between the fine and coarse particles or the shape of the coarse particles.

Fig. 5a shows the mobility of flows on a 10° slope consisting of binary mixtures of fine and coarse particles: $140\mu\text{m}$ ballotini and slab-like glass rafters; $90\mu\text{m}$ ballotini and slab-like glass rafters; $140\mu\text{m}$ ballotini and slab-like glass double rafters; $140\mu\text{m}$ ballotini and 20mm glass spheres; and $140\mu\text{m}$ ballotini and 8mm glass spheres (see Table 1 for the dimensions of the fine and coarse particles used in all experiments). The flows with non-spherical coarse particles show a sharp peak in mobility at a fine particle mass fraction of 0.3, with scaled downslope mobility (M/M_0) of about 2.5 for the flow with the larger fine and coarse particles and about 3.5 for the flow consisting of the smaller fine and coarse particles. The flows with spherical coarse particles show different behaviour because the coarse particles are able to roll independently of the motion of the fine particles. For fine particle mass fractions less than 0.8 (in experiments with 20mm diameter spheres as the coarse particles) and 0.6 (in experiments with 8mm diameter spheres as the coarse particles), the coarse particles roll to the end of the tank and the scaled downslope mobility $M/M_0=1$. For fine particle mass fractions greater than these values, the coarse particles do not move independently of the fine particles and the scaled downslope mobility is reduced. Fig. 5b shows the mobility of flows on a 10° slope consisting of binary mixtures of fine and coarse particles of different composition: $140\mu\text{m}$ PVC beads and slab-like glass rafters; $140\mu\text{m}$ ballotini and sub-spherical gravel; and

$140\mu\text{m}$ silicon carbide powder and slab-like glass rafters (see Table 1). The flows show a broader peak in mobility between a fine particle mass fraction of 0.2 to 0.4, with scaled downslope mobility (M/M_0) of about 2 for the flow consisting of the lower density spherical PVC beads as the fine particles and about 2.5 for the flow consisting of the spherical glass ballotini and sub-spherical gravel. The peak is broader when the coarse particles are more nearly spherical, and in this case their surface roughness dimension is also much smaller than the fine particle diameter. In general, the enhancement of flow mobility in flows containing a mixture of fine and coarse particles, with peak mobility at a fine particle mass fraction of about 0.3, appears to be independent of differences in fine particle size, density and shape, and coarse particle size and shape, within the range of values used in these experiments.

Fig. 5c and d show the mobility of flows consisting of binary mixtures of two-dimensional glass rafters as the coarse particles and various fine particles on a 20° slope. Fig. 5c shows the mobility of flows where there is no density difference between the fine and coarse particles; the flows with non-spherical coarse particles show a peak in mobility at a fine particle mass fraction of between 0.2 and 0.4, with scaled downslope mobility (M/M_0) ranging from about 3 to about 3.5. Flows with spherical coarse particles show similar behaviour to that on the shallower slope (Fig. 5a). Fig. 5d shows the mobility of flows where the fine particles are different in shape and density. The scaled downslope mobility (M/M_0) is about 3 for flows in which the fine particles are angular silicon carbide, and about 5.5 for flows in which the fine particles are spherical PVC beads. The peak in mobility is broader for flows of particle mixtures where there is a density contrast between the fine and coarse particles.

4. Interpretation and analysis of flow mobility

The experiments described here vary the fine material component of the granular mixture but maintain the same total mass. Since the coarse particles typically have a higher porosity than the fine particles, the volume and hence initial aspect ratio a (=initial height/lock length) of the material unavoidably increases as ψ decreases. This effect alone is known to produce increased run out of monodisperse materials over horizontal planes [29–33] but does not explain the enhanced *mobility* observed here which is the *ratio* of the downslope position of the centre of mass of the deposit and the initial height of the centre of mass. In fact, applying the observed scaling law for two-dimensional monodisperse lock release [31–33] (run

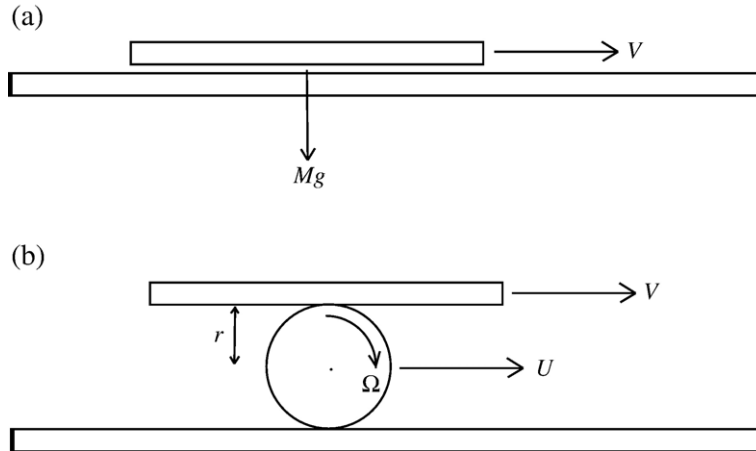


Fig. 6. Schematic diagram of the motion of a slab-like coarse particle in (a) the absence and (b) the presence of a spherical fine particle.

out/lock length $\sim a^{2/3}$ which we have observed also on sloping planes for aspect ratios of interest here) and normalising by the initial height actually predicts $M \sim a^{-1/3}$ – a decrease in mobility as ψ decreases from 1. Therefore, these bidisperse results presented above are fundamentally different from the monodisperse results [31–33].

We interpret the experimental results in terms of changes in frictional regime in the flow when the particle mixture consists of mostly coarse material – hereafter referred to as Regime I ($0 < \psi \leq 0.2$), a mixture of fine and coarse – hereafter Regime II ($0.2 \leq \psi \leq 0.7$), and mostly fine material – hereafter Regime III ($0.7 \leq \psi < 1$). We hypothesize that the dominant source of frictional dissipation of energy is different in the two limiting Regimes I and III and develop simple model calculations to illustrate this.

At low fine material mass fractions (Regime I), the experimental flows exhibit increasing run out distance as the proportion of fine material is increased. We suggest that the dominant effect is the rolling of the fine particles which acts to lubricate the motion of the coarse particles. The fine particles will naturally migrate in between the coarse particles to lubricate their movement and also under gravity to the base of the flow via kinetic sieving [15], an effect which does not depend strongly on the relative density of the fine and coarse material. Once at the base, the fine particles can alleviate the frictional losses with the base by reducing the frictional contact area (especially if the coarse particles have planar surfaces) as well as acting like ‘rollers’.

As a general principle, frictional losses in a granular flow are reduced if particles experience rolling rather than sliding contacts. This can be seen by considering a simple illustrative model of the motion of a coarse slab-

like particle in the absence or presence of fine spherical particles (Fig. 6). For a slab-like particle of mass M sliding on a horizontal flat surface at velocity V , the rate of energy dissipation $L = \mu MgV$, where μ is the coefficient of friction and g is the acceleration due to gravity (Fig. 6a). For the same particle supported on a spherical particle of mass m and radius r , the rate of energy dissipation is given by

$$L = \mu(M + m)g|U - r\Omega| + \mu Mg|V - U - r\Omega|,$$

where U and Ω are the velocity and angular velocity of the fine particle (Fig. 6b). If we define the degree of rolling of the spherical particle $\lambda = (r\Omega)/U$ and the velocity ratio $\Gamma = (2U)/V$, we find

$$L = \mu(M + m)g \frac{1}{2} \Gamma V |1 - \lambda| + \mu Mg V |1 - \frac{1}{2} \lambda - \frac{1}{2} \Gamma \lambda|.$$

From this expression, we can see that the rate of energy dissipation is uniquely made to vanish if $\Gamma = \lambda = 1$, that is when the degree of rolling matches the velocity ratio at 1.

Rolling motion does not require perfectly spherical particles. Consider a spherical particle on a slope (Fig. 7a), with θ being the angle between the weight of the particle acting vertically through the centre of mass, and the point at which the particle pivots in contact with the underlying surface, P . For rolling motion, the angle θ must be positive, with the coefficient of friction of the surface being sufficiently large to inhibit sliding motion. On the same slope, an irregularly shaped object may not roll (Fig. 7b), although the tendency for it to roll increases with the slope angle (Fig. 7c).

At low fine material mass fraction (Regime I), the experimental results (Fig. 5) are consistent with our

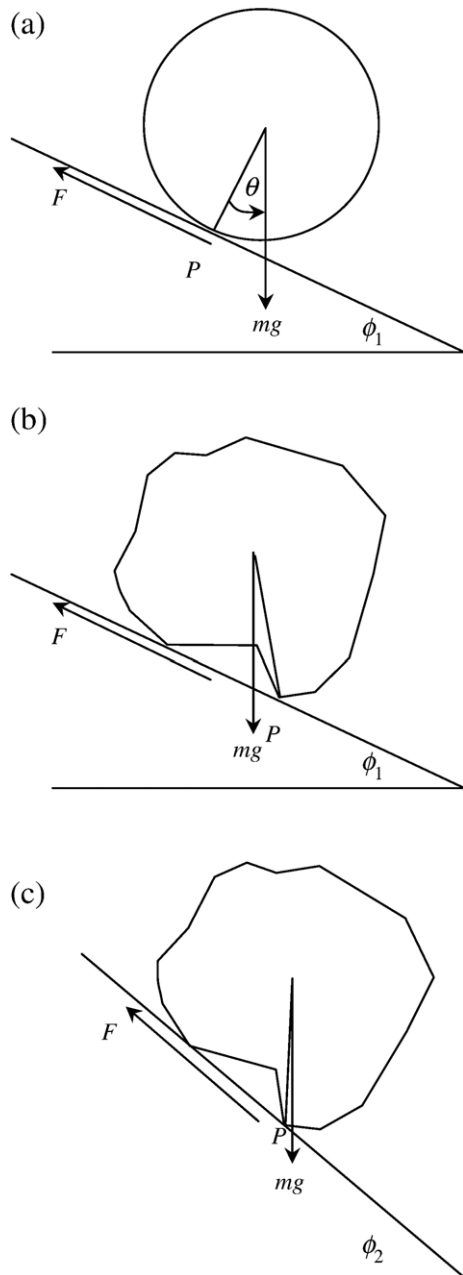


Fig. 7. Schematic diagram of rolling motion on a slope: (a) spherical particle; (b) irregular particle on a shallow slope; (c) irregular particle on a steeper slope.

interpretation. As the mass fraction of fine particles ψ increases from 0, the run out distance increases significantly for all combinations of fine and coarse particles on both slopes. As the mass fraction of fine particles increases, a greater proportion of the coarse particles are completely supported by the fine particles, reducing the overall friction on the flow and increasing the run out distance.

It is clear that once the mass fraction of fine particles becomes significant, their effect becomes more complicated than just acting as a coarse particle lubricant. Frictional effects between the fine particles themselves should become significant and must dominate as ψ tends to 1. Therefore, in Regime III, we expect inter-particle friction to be the primary source of energy loss which limits mobility. A simple idea to model this regime is to assume that the frictional loss experienced by the granular flow is directly proportional to the surface area of the particles exposed for frictional contact. The effect of substituting a coarse particle for the same mass of fine particles would then be to reduce the surface area of particles available for interactions, equivalent to a ‘locked’ region that experiences lower frictional interactions than regions where particles are free to interact. We explore the implications of this heuristic model for our experimental results by considering the simplified situation of a bidispersed particle mixture in which frictional losses occur by particle interaction, and the flow run out distance is inversely correlated to the frictional loss although the exact relationship is unknown.

For a flow of mass m consisting of all fine particles of surface area S_f , volume V_f and density ρ_f , we suppose that on average the total frictional loss is equal to nS_fF , where n is the total number of particles, $n = m/[V_f\rho_f]$, and F is the frictional force per surface area of the particles. For a flow of the same total mass consisting of mainly fine particles of number n_f and a few coarse particles of number n_c , density ρ_c , volume V_c and surface area S_c , but with the same frictional force per unit surface area, the total frictional force relative to that for a flow consisting purely of fine particles is given by

$$R = \frac{S_f n_f F + S_c n_c F}{S_f n F}.$$

The mass fraction of fine particles is given by $\psi = n_f/n$, while mass conservation for this flow yields

$$n = n_f + \frac{\rho_c V_c}{\rho_f V_f} n_c n.$$

Hence the frictional forces relative to that for a flow purely of fine particles is given by

$$R = 1 + \left(\frac{S_c \rho_f V_f}{S_f \rho_c V_c} - 1 \right) (1 - \psi).$$

We note the ratio of the volume of a particle to its surface area gives a length-scale which is indicative of its size and we denote the ratio of these sizes by $\gamma = (V_f/S_f)/(V_c/S_c)$. In the special case of spherical fine and coarse

Table 2
Comparison of observations of downslope mobility with model predictions

Experiment	γ	χ	$\chi\gamma-1$	$d(M/M_1)/d\psi^a$	
				10° slope	20° slope
140 μm silicon carbide+rafters	0.023	1.30	-0.970	-0.09 (-0.04)	-0.32 (-0.21)
140 μm ballotini+rafters	0.023	1	-0.970	-0.14 (-0.15)	-0.36 (-0.50)
140 μm ballotini+8mm glass spheres	0.018	1	-0.982	-0.18 (-0.04)	^{-b} (-0.76)
90 μm ballotini+rafters	0.015	1	-0.985	-0.23 (-0.21)	-1.25 (-1.26)
140 μm ballotini+double rafters	0.013	1	-0.987	-0.37 (-0.49)	-1.26 (-1.50)
140 μm ballotini+gravel	^c	0.98	-	-	-
140 μm PVC+rafters	0.023	0.57	-0.987	0.0 (0.0)	0.0 (0.0)
140 μm ballotini+20mm glass spheres	0.007	1	-0.993	-0.63 (-0.66)	^{-b}

$d(M/M_1)/d\psi$ is inversely correlated with $dR/d\psi$, which is equal to $-(\chi\gamma-1)$, as predicted by the model.

^a Calculated by linear curve fit to experimental data from $0.8 \leq \psi < 1$. Values in parentheses correspond to $0.9 \leq \psi < 1$.

^b Under these conditions, the coarse spherical particles rolled away from the flow deposit to the edge of the experimental apparatus.

^c Gravel particles ranged in diameter from 10mm to 20mm so it was not possible to calculate a representative γ value.

particles, this parameter is equal to the ratio of the radius of a fine particle to the radius of a coarse particle ($\gamma = r_f/r_c$). We also denote the ratio of the densities by $\chi = \rho_f/\rho_c$ and thus we find that

$$R = 1 + (\chi\gamma-1)(1-\psi).$$

This simple model is only appropriate when ψ close to one. However it does make two predictions. Firstly a flow containing a few coarse particles and mainly fine particles will run out further than a flow containing all fine particles if $\chi\gamma < 1$. Secondly and more specifically, flows with the smallest values of $(\chi\gamma-1)$ should show the greatest increase in run out distance when the proportion of coarse particles in the flow is increased from zero.

Table 2 shows a comparison of how this heuristic model suggests the downslope mobility M (normalised by the downslope mobility M_1 at $\psi=1$) changes with ψ near 1 (Regime III) with the experimental observations on the 10° and 20° slopes. The experimental results are consistent with the model predictions in that the order implied by $R=1+(\chi\gamma-1)(1-\psi)$ is the order of increase of mobility seen in the experiment. At high fine material mass fractions, the flow run out distance increases with decreasing ψ and with the ratio of the size of the coarse particles to the size of the fine particles, on both 10° and 20° slopes. On the lower slope, the run out distance increases with the ratio of the density of the coarse particles to the density of the fine particles, with the exception of the PVC particles. These particles have a high angle of internal friction (see Table 1), which may be due to electrostatic forces between the particles. On the steeper slope, the flow run out distance increases with the ratio of density of the coarse particles to density of the fine particles, for all experimental materials.

At some intermediate proportion of fine to coarse particles (in Regime II), there will be a maximum run out distance, although our simple physical reasoning cannot be used to infer the fine particle mass fraction at which this occurs. In our experiments, the maximum run out distance is observed at a fine material mass fraction $\psi \approx 0.3$. We now discuss our observations of flow deposits to identify key features of the mobility of flows containing a mixture of particle sizes.

5. Discussion

In our experimental flows that exhibit high mobility ($\psi=0.3$), the mass deposition of fine and coarse particles is most similar at any given position in the deposit, whereas the mass deposition of fine and coarse particles is dissimilar for flows with low mobility (Fig. 4). There appears to be less segregation between the particle sizes along the length of the deposit of a flow with high mobility compared to a flow with lower mobility. In high mobility flows, it appears that fine particles are transported with the coarse particles, and can thus lubricate their interaction with each other and the underlying surface via mechanisms such as rolling motion. The precise details of particle interactions are unknown, and we cannot make observations of fine particle motion within these flows. However, these observations suggest that particle interactions are significant within flows of high mobility where there are large differences in the sizes of the fine and coarse particles. The extent of gravitational slumps of mono-dispersed particles has been widely recognised to be strongly positively correlated with the initial aspect ratio of the granular pile [29–33]. For bidispersed materials, this scaling would predict that the flow downslope mobility (as defined in this study) would decrease with

initial aspect ratio, the reverse trend to our experimental observations. We suggest that these observations indicate a fundamentally different control on the propagation of flows containing more than one particle size as compared with flows of monodispersed materials.

The enhanced mobility of flows consisting of fine and coarse particles at fine particle mass fraction of about 0.3 appears to be independent of fine particle density over the range of our experimental conditions. This observation is consistent with observations of particle segregation in granular flows [15,16], which also arise from particle interactions. Fine particle segregation to the base of granular chute flows is widely observed in experimental studies [15,16,13,36] and would enhance the lubrication of the coarse particle motion against the underlying surface. In our experiments, the fine particles are of comparable dimension to the roughness of the tank base and the two-dimensional coarse slabs. In contrast to studies using monodispersed particles in which this condition produced a minimum flow mobility [24], we find that the presence of fine particles can enhance the flow mobility. Further experimental work is required to identify the interactions between fine particles and the surface roughness, but our observations are consistent with rolling motion of fine particles that can fill spaces in the surface roughness of the coarse particles and the underlying surface. In experiments where the coarse particles have a surface roughness dimension much smaller than that of the fine particles, we find that the peak in flow mobility extends over a greater range of fine particle mass fraction than for experiments where the fine particle diameter and surface roughness dimension are comparable (Fig. 5). Further experiments with a wider range of fine particle size and surface roughness dimension are required to understand the precise details of the fine and coarse particle interaction on these length scales.

Our observations of higher mobility (and hence lower dissipation) in flows of particle mixtures with a fine particle mass fraction between about 0.2 and 0.4 are consistent with other experimental observations of granular dynamics in which fine and coarse particles co-exist [17,18]. In these other studies, the particle sizes are very different to those in our experiments, so there is no geometrical reason why this range of fine particle mass fractions should correspond to a minimum dissipation state. Further experimental observations of particle interactions in these flows are required to understand why this fine particle mass fraction is significant.

We have investigated the variation in mobility of granular flows containing fine and coarse particles using

heuristic models to illustrate the increase in mobility of flows that contain a mixture of fine and coarse particles as compared with flows that contain either all fine or all coarse particles. We have analysed a model flow containing coarse and fine particles considering the coarse particles as regions of ‘locked’ flow in which fine particle interactions are eliminated. We find that predictions of the increase in flow mobility in the limit where the mass fraction of fine particles is close to unity are consistent with the experimental observations. In the opposite limit, we have shown explicitly, using model calculations, that increasing the proportion of rolling to sliding in particle motion reduces energy loss. These observations cannot be used to quantitatively analyse the experimental data, but emphasize that rolling motion may be important in flows of fine and coarse particles where the fine particle size is very much smaller than the coarse particle size, as in our experiments. In the absence of complete parameterisations for these particle interactions in granular flow, these heuristic approaches represent the only available investigative tools.

6. Implications for geophysical granular flow

Increased granular flow mobility due to interaction of fine and coarse material could form an important influence on the dynamics of some landslides and block-and-ash pyroclastic flows. Although these small-scale experiments do not show the order of magnitude increase in run out observed in terrestrial ‘long-run out’ landslides [35], this mechanism may still provide enhanced mobility in flows which contain very coarse and very fine material. Dry rockslide deposits commonly contain fine material (typically sub-spherical particles with diameters in the range 10^{-2} to 1 cm) [1], which, if not initially present, can be generated as a consequence of collisions and grinding of smaller material by larger material. The experimental observations in this study suggest that the degree of segregation of large and small particle sizes along the deposit may be indicative of the mobility of the flow. An important next step will be to make measurements of both vertical and horizontal segregation in deposits from large geophysical granular flows such as rockslides and block-and-ash pyroclastic flows.

Experimental studies of slumping of monodispersed granular piles onto horizontal surfaces [29–31] suggest that the run out ratio of the flow is independent of its initial volume and have emphasized the aspect ratio (height/length) of the granular pile as the key control

on run out. The experimental observations presented in this study also suggest that the controls on propagation of flows containing more than one particle size are fundamentally different from those containing a single size of particle. It is becoming apparent that prediction of the run out length and dynamics of geophysical granular flows will only be fully realisable once the interaction of particles of different sizes and the control this provides on the operation and onset of frictional forces are understood. Environmentally, hazard prediction studies will benefit from improved understanding of rolling particle motion, and industrially, exploiting the enhanced mobility of granular mixtures may offer savings in solids conveying costs. The challenges ahead in this research area are the investigation of the internal structure of laboratory flows and the development of constitutive laws for rolling motion and enduring frictional contacts within granular flows.

Acknowledgements

The authors gratefully acknowledge stimulating and useful discussions with R.S.J. Sparks and O. Roche, and constructive and helpful reviews by two anonymous reviewers.

References

- [1] B. Voight (Ed.), *Rockslides and Avalanches: I. Natural Phenomena*, Elsevier, New York, 1978, 833 pp.
- [2] P.D. Cole, E.S. Calder, R.S.J. Sparks, A.B. Clarke, T.H. Druitt, S. R. Young, R.A. Herd, C.L. Harford, G.E. Norton, Deposits from dome-collapse and fountain-collapse pyroclastic flows at Soufriere Hills Volcano, Montserrat, The Eruption of the Soufriere Hills Volcano, Montserrat, from 1995–1999, *Geol. Soc. Lond. Mem.*, vol. 21, 2002, pp. 231–262.
- [3] H.L. Hartman, *Introductory Mining Engineering*, Wiley-Interscience, New York, 1987, 622 pp.
- [4] R.H. Perry, C.H. Chilton (Eds.), *Chemical Engineers Handbook*, 5th ed., McGraw-Hill Kogakusha, Tokyo, 1973, 1131 pp.
- [5] M.E. Mobius, B.E. Lauderdale, S.R. Nagel, H.M. Jaeger, Size separation of granular particles, *Nature* 414 (2001) 270.
- [6] T. Shinbrot, The Brazil nut effect – in reverse, *Nature* 429 (2004) 352–353.
- [7] R. Jullien, P. Meakin, A mechanism for particle-size segregation in three dimensions, *Nature* 344 (1990) 425–427.
- [8] J. Duran, J. Rajchenbach, E. Clement, Arching effect model for particle-size segregation, *Phys. Rev. Lett.* 70 (1993) 2431–2434.
- [9] J.B. Knight, H.M. Jaeger, S.R. Nagel, Vibration induced size separation in granular media – the convection connection, *Phys. Rev. Lett.* 70 (1993) 3728–3731.
- [10] W. Cooke, S. Warr, J.M. Huntley, R.C. Ball, Particle size segregation in a two-dimensional bed undergoing vertical vibration, *Phys. Rev.*, E 53 (1993) 2812–2822.
- [11] F.J. Muzzio, B.J. Glasser, T. Shinbrot, Powder technology in the pharmaceutical industry: the need to catch up fast, *Powder Technol.* 124 (2002) 1–7.
- [12] A.P.J. Breu, H.-M. Ensner, C.A. Kruegel, I. Rehberg, Reversing the Brazil-nut effect: competition between percolation and condensation, *Phys. Rev. Lett.* 90 (2003) 014302.
- [13] J.A. Drahn, J. Bridgewater, The mechanisms of free surface segregation, *Powder Technol.* 36 (1983) 39–53.
- [14] H.A. Makse, S. Havlin, P.R. King, H.E. Stanley, Spontaneous stratification in granular mixtures, *Nature* 386 (1997) 379–382.
- [15] S.B. Savage, C.K.K. Lun, Particle size segregation in inclined chute flow of dry cohesionless granular solids, *J. Fluid Mech.* 189 (1988) 311–335.
- [16] J.W. Vallance, S.B. Savage, Particle segregation in granular flows down chutes, IUTAM Symposium on Segregation in Granular Flows, *Solid Mechanics and its Applications Series*, The Netherlands, 2001, pp. 31–51.
- [17] S. Thevanayagam, M. Fiorillos, J. Liang, Effect of non-plastic fines on the undrained cyclic strength of silty sands, in: R.Y.S. Pak, J. Yamamura (Eds.), *Soil Dynamics and Liquefaction*, A.S.C.E. Geotechnical Special Publication, vol. 107, 2000, pp. 146–154.
- [18] Y.P. Vaid, Liquefaction of silty soils, *A.S.C.E. Geotech. Spec. Publ.* 44 (1994) 1–16.
- [19] J.F. Wambugh, C. Reichhardt, C.J. Olson, Ratchet-induced segregation and transport of non-spherical grains, *Phys. Rev.*, E 65 (2002) 031308.
- [20] F.X. Riguidel, A. Hansen, D. Bideau, Gravity-driven motion of a particle on an inclined plane with controlled roughness, *Europhys. Lett.* 28 (1994) 13–18.
- [21] F.X. Riguidel, R. Jullien, G.H. Ristow, A. Hansen, D. Bideau, Behaviour of a sphere on a rough inclined plane, *J. Phys.*, I 4 (1994) 261–272.
- [22] G.H. Ristow, F.X. Riguidel, D. Bideau, Different characteristics of the motion of a single particle on a bumpy inclined line, *J. Phys.*, I 4 (1994) 1161–1172.
- [23] C. Anciay, P. Evesque, P. Coussot, Motion of a single bead on a bead row: theoretical investigations, *J. Phys.*, I 6 (1996) 725–751.
- [24] C. Goujon, N. Thomas, B. Dalloz-Dubrujeaud, Monodisperse dry granular flows on inclined planes; role of roughness, *Eur. Phys. J.*, E Soft Matter 11 (2003) 147–157.
- [25] M. Babic, H.H. Shen, H.T. Shen, The stress tensor in antigranulocytes shear flows of uniform deformable disks at high solids concentrations, *J. Fluid Mech.* 219 (1990) 81–118.
- [26] B. Miller, C. O'Hern, R.P. Behringer, Stress fluctuations for continuously sheared granular materials, *Phys. Rev. Lett.* 77 (15) (1996) 3110–3113.
- [27] J. Rajchenbach, Granular flows, *Adv. Phys.* 49 (2000) 229–256.
- [28] G.R.D. Midi, On dense granular flows, *Eur. Phys. J.*, E Soft Matter 14 (4) (2004) 341–356.
- [29] G. Lube, H.E. Huppert, R.S.J. Sparks, M.A. Hallworth, Axisymmetric collapses of granular columns, *J. Fluid Mech.* 508 (2004) 175–199.
- [30] E. Lajeunesse, A. Mangeney-Castelnau, J.P. Vilotte, Spreading of a granular mass on a horizontal plane, *Phys. Fluids* 16 (7) (2004) 2371–2381.
- [31] N.J. Balmforth, R.R. Kerswell, Granular collapse in two dimensions, *J. Fluid Mech.* 538 (2005) 399–428.
- [32] E. Lajeunesse, J.B. Monnier, G.M. Homsy, Granular slumping on a horizontal surface, *Phys. Fluids* 17 (2005) 103302.

- [33] G. Lube, H.E. Huppert, R.S.J. Sparks, A. Freundt, Collapses of two-dimensional granular columns, *Phys. Rev., E* 72 (2005) 041301.
- [34] O. Roche, M.A. Gilbertson, J.C. Phillips, R.S.J. Sparks, Experiments on deaerating granular flows and implications for pyroclastic flow mobility, *Geophys. Res. Lett.* 29 (2002) 1792.
- [35] W.B. Dade, H.E. Huppert, Long runout rockfalls, *Geology* 26 (1998) 803–806.
- [36] G. Felix, N. Thomas, Evidence of two effects in the size segregation process in dry granular media, *Phys. Rev., E* 70 (5) (2004) 051307.